ELSEVIER

NeuroImage

www.elsevier.com/locate/ynimg
NeuroImage xx (2005) xxx – xxx

3D mapping of ventricular and corpus callosum abnormalities in HIV/AIDS

Paul M. Thompson,[a,*] Rebecca A. Dutton,[a] Kiralee M. Hayashi,[a] Allen Lu,[a] Sharon E. Lee,[a] Jessica Y. Lee,[a] Oscar L. Lopez,[b] Howard J. Aizenstein,[c] Arthur W. Toga,[a] and James T. Becker[b,c,d]

[a]*Laboratory of Neuro Imaging, Dept. of Neurology, UCLA School of Medicine, 635 Charles E. Young Drive South, Suite 225E, Los Angeles, CA 90095-7332, USA*
[b]*Dept. of Neurology, Univ. of Pittsburgh, Pittsburgh, PA 15260, USA*
[c]*Dept. of Psychiatry, Univ. of Pittsburgh, Pittsburgh, PA 15260, USA*
[d]*Dept. of Psychology, Univ. of Pittsburgh, Pittsburgh, PA 15260, USA*

Received 14 August 2005; revised 30 November 2005; accepted 30 November 2005

Objective: **40 million people worldwide are now infected with HIV/AIDS, an illness that often leads to rapidly progressing dementia and death. Even so, little is known about how AIDS affects the brain. Using computational anatomy techniques, we mapped how AIDS impacts the corpus callosum (CC) and ventricular system, two systems that show prominent changes on MRI. We (1) identified regions with greatest differences between AIDS patients and healthy controls and (2) correlated specific 3D patterns of structural differences with measures of immune system deterioration and cognitive decline.**
Methods: **51 3D brain MRI scans from 30 non-demented AIDS patients (age: 43.4 years ± 7.6 SD) and 21 HIV-seronegative controls (age: 39.5 years ± 12.2) were aligned to ICBM standard space. 3D surface mesh reconstructions of the lateral ventricles and CC were spatially averaged and compared across diagnostic groups. Structural alterations were correlated with viral load, T cell counts, and cognitive impairment.**
Results: **Statistical maps revealed the 3D profile of ventricular expansion and callosal thinning in AIDS. Specific 3D ventricular changes were linked with immune system decline (CD4+ T cell counts; $P < 0.001$) and cognitive impairment ($P < 0.009$), but not viral load. Frontal horn maps distinguished AIDS patients from controls better than occipital and temporal horn measures. T cell decline linked with callosal thinning in anterior regions connecting frontal areas with greatest cortical atrophy.**
Conclusion: **These maps (1) reveal how brain changes in HIV/AIDS relate to immune decline and impaired cognition, and, after further validation and testing, (2) may offer possible neuroimaging markers for anti-viral drug trials, which gauge how well treatments oppose disease progression in the brain.**

Introduction

HIV infection is a worsening epidemic, with 40 million people now infected, and 5 million new cases in 2004 alone (UNAIDS, 2004). Brain mapping in HIV/AIDS is of interest because little is known about how HIV infection progresses in the central nervous system. Highly active anti-retroviral therapy (HAART) was introduced as a treatment for AIDS in the late 1990s and has bolstered the immune system against opportunistic infections and cancers in HIV-infected patients. Despite this success, anti-viral treatments may not protect the brain from HIV-related neurodegeneration. Most treatments have difficulty crossing the blood brain barrier, and the CNS becomes, in effect, a sanctuary or reservoir for the HIV virus (see Cysique et al., 2004). The use of multiple CNS-penetrating components does not appear to protect the CNS from the effects of the infection. Even though opportunistic infections have diminished as a major cause of death, HIV encephalitis is now more prevalent (Neuenburg et al., 2002; Langford et al., 2003). The benefits of HAART should not be understated, and HIV-associated dementia has decreased by 50% since the introduction of HAART (Sacktor et al., 2002). Even so, cognitive disorders and neuropsychological problems are now more common. Around 40% of HIV patients report cognitive impairments ranging from minor cognitive motor disorders (MCMD) to HIV-associated dementia. For many, neurologic symptoms are the first sign of HIV infection (Levy et al., 1986).

Brain atrophy is seen clearly in AIDS patients with MRI, with that found in the striatum, hippocampus, white matter, and posterior cortex correlating with cognitive decline even in HIV patients without dementia (Patel et al., 2002; Becker et al., in press, submitted for publication). This atrophy begins in the medically asymptomatic stage and later accelerates (Stout et al., 1998; Heyes et al., 2001; Archibald et al., 2004). It is therefore of interest to find

* Corresponding author. Fax: +1 310 206 5518.
E-mail address: thompson@loni.ucla.edu (P.M. Thompson).
Available online on ScienceDirect (www.sciencedirect.com).

1053-8119/$ - see front matter © 2005 Elsevier Inc. All rights reserved.
doi:10.1016/j.neuroimage.2005.11.043

ways to gauge brain integrity in HIV-infected patients and to understand how MRI-based measures relate to systemic changes in viral load, immune system integrity, and cognitive decline. Surrogate markers of disease burden provided by brain mapping may be beneficial for drug trials, potentially reducing the number of subjects or duration of follow-up required to establish whether CNS degeneration is being delayed or averted.

In older studies, simple 2D planimetric measures of the ventricles, or bicaudate ratios (Hestad et al., 1993) were often used to gauge HIV disease progression and poor prognosis. Viral load is highest in the caudate nuclei, which lie adjacent to ventricular spaces enriched in the virus, and the basal ganglia become severely atrophied in AIDS. Caudate atrophy correlates with reduced motor speed in advanced AIDS, independent of the degree of immunosuppression and overall brain atrophy (Kieburtz et al., 1996). AIDS patients also have reduced frontal and parietal gray matter volumes (by around 8%, on average), and, within the cortex, atrophy affects sensorimotor regions the most (Thompson et al., 2005a,b). White matter abnormalities are also common in AIDS patients, including diffuse or patchy white matter lucencies on T2-weighted images (Navia and Gonzalez, 1997; see, e.g., Thurnher et al., 2000, for examples). Subcortical and cortical deficits have also been identified with PET (Rottenberg et al., 1996), SPECT (Sacktor et al., 1995), proton MR spectroscopy (Chang et al., 2004; Ernst and Chang, 2004), and diffusion tensor imaging (Filippi et al., 2001; Pomara et al., 2001; Ragin et al., 2004).

As HIV-related atrophy does not affect the brain uniformly, we set out to map the spatial pattern of structural alterations in two systems where changes are clear on MRI and easy to measure: the lateral ventricles and corpus callosum (CC). We sought specific anatomical measures that correlated best with diagnosis, markers of immune suppression, and viral load, as well as cognitive impairment. Some prior studies have revealed interesting relationships between volumetric measures of global or regional brain atrophy and neurocognitive function in the course of HIV infection, including longitudinal studies that have correlated specific patterns of cognitive decline over time with progressive changes in MR volumetric ratios (Hall et al., 1996). Computational anatomy techniques however – such as surface modeling – have not been applied before to study AIDS, but they have been effective in modeling hippocampal and ventricular alterations in Alzheimer's disease and schizophrenia (Thompson et al., 2004a,b; Narr et al., 2004; Csernansky et al., 2005; Wang et al., 2003). Surface-based models of anatomy can be averaged and compared statistically across subjects and groups, revealing systematic patterns of brain change in 3D. Applying them to these AIDS patients, we expected to be able to map greatest ventricular expansion in the frontal horns, which lie adjacent to caudate regions with highest viral load (Stout et al., 1998). We also expected that our maps would reveal greatest thinning in the midbody regions of the corpus callosum, as these carry fibers from the sensorimotor cortices that are most atrophied in HIV/AIDS (Thompson et al., 2005a,b).

Methods

Subjects

51 Subjects were scanned with MRI, of whom 30 had CDC-defined (Center for Disease Control, 1992) AIDS (i.e., CDC-Stage C; mean age: 43.4 years ± 7.6 SD). 21 were HIV-seronegative controls (age: 39.5 years ± 12.2) with similar HIV-related risk factors to the AIDS patients. None had HIV-associated dementia (patients' mean CD4+ T cell count was 436.0 ± 301.0; patients' mean $\log_{10}$ viral load was 2.63 ± 1.28 RNA copies per milliliter blood plasma). Viral load was measured with an ultra-sensitive assay (Roche Pharmaceuticals) with a lower detectability limit of 50 copies/ml.

Health care providers in Allegheny County (Pennsylvania) served as a sentinel network for recruitment; AIDS patients seen in the sentinel offices and clinics were approached for participation by their treating physician. All AIDS patients were eligible to participate, excluding only those with a history of central nervous system opportunistic infections, lymphoma, or stroke. All subjects signed Informed Consent forms before participating in the research (which had been approved by the University of Pittsburgh Institutional Review Board). Demographic data for this cohort are reported in Becker et al. (in press, submitted for publication). This sample extends a prior sample of 40 subjects (26 with AIDS and 14 controls) for whom cortical thickness maps were reported in Thompson et al. (2005a,b).

Neurobehavioral assessment

Each subject underwent a detailed neurobehavioral assessment prior to their MRI scan, involving a neurological exam, psychosocial interview, and neuropsychological testing. The neurological exam was conducted by a Research Nurse supervised by a behavioral neurologist (O.L.L.) and covered the entire nervous system. The motor component of the Unified Rating of Parkinsonism Scale (Fahn et al., 1987) measured the severity of extrapyramidal signs. Each participant underwent a psychosocial interview, including (i) a semi-structured psychiatric interview, modified from the Structured Clinical Interview for DSM-III-R (SCID; Spitzer et al., 1989) administered by a trained interviewer; (ii) the Brief Symptom Inventory (Derogatis, 1992) and the Neuropsychiatric Inventory (NPI; Cummings et al., 1994) to assess subclinical psychiatric symptoms; and (iii) Heaton's Patient's Assessment of Own Function questionnaire (Heaton, 1981) and the Modified Instrumental Activities of Daily Living scale (Lawton and Brody, 1969) to evaluate specific symptoms of cognitive decline and their impact on daily living. Neuropsychological evaluation included measures from multiple cognitive domains, sensitive to AIDS-related cognitive impairments (Becker et al., 2004). Table 1 shows a summary of the subjects' neuropsychological data. Subjects were also designated as Impaired or Unimpaired (Table 1), based on a comprehensive review of the cognitive data by a neuropsychologist (J.B.) blinded to information on whether each subject was HIV positive or negative. This binary outcome variable (Impairment), while not specific to any one cognitive domain, is sensitive to AIDS-related cognitive impairments (Becker et al., 2004). In the maps that correlate impairment with maps of callosal thinning and ventricular expansion, this binary measure of impairment was used for computing correlations with the anatomical measures.

MRI scanning and tissue classification

3D volumetric SPGR (spoiled gradient echo) MRI scans of the brain were acquired identically for all 51 subjects (256 × 256 × 124 matrix; 24 cm FOV; 1.5 mm slices, zero gap; flip angle, 40°, TE = 5, TR = 25). All 51 individual brain volumes were rigidly re-

Table 1
Neuropsychological test scores in AIDS patients and controls

	Controls				AIDS Patients			
	Unimpaired		Impaired		Unimpaired		Impaired	
	Mean	SD	Mean	SD	Mean	SD	Mean	SD
Speed score[a]	0.61	0.50	−0.77	1.19	−0.33	1.63	−2.14	2.66
Fluency score[a]	0.08	0.98	−0.38	0.81	0.03	0.86	−0.97	0.99
Reaction time score[a]	−0.12	1.28	−0.41	0.66	−0.38	0.88	−0.24	0.67
WAIS-R vocabulary subtest [1][b]	11.91	3.08	8.20	2.28	10.47	4.09	7.33	4.23
FSIQ estimated from North American Adult Reading Test [2][c]	117.94	7.86	101.52	12.78	112.13	10.08	104.98	17.53

This table reports the mean scores and standard deviations for a range of standard neuropsychological tests administered to the subjects in this study. Scores are presented separately for patients and controls who were designated as impaired and unimpaired, based on a comprehensive review of the cognitive data by a neuropsychologist (J.B.) blinded to information on whether each subject was HIV positive or negative. Factor analysis revealed a latent structure that included the domains of psychomotor speed, verbal fluency, and reaction time reported here. These scores are adjusted, i.e. they represent the difference between the observed standardized score (in z units) and the scores that would be predicted based on age, education and sex (based on multiple regression of all the data from the HIV-negative controls). References: [1]. Wechsler, D. (1981) *Wechsler Adult Intelligence Scale*—Revised. New York: *The Psychological Corporation*; [2]. Spreen, O., Strauss, E. (1998) *A Compendium of Neuropsychological Tests*, New York, Oxford University Press; [3]. Lezak, M. (1995) *Neuropsychological Tests*, 3rd Edition, New York. Oxford University Press.

[a] Scores for psychomotor speed, verbal fluency, and reaction time were estimated by factor analysis of the scores from the Grooved Pegboard test, the Trailmaking test (parts A and B), the Controlled Oral Word Association (and Category Fluency) test, and the Continuous Performance Test.

[b] Age-scaled Scores for the WAIS-R vocabulary subtest are reported; these are highly correlated with IQ.

[c] FSIQ (Full-scale Intelligence Quotient) was estimated from the North American Adult Reading Test [2].

oriented into the standardized coordinate system of the ICBM-53 average brain, correcting for head tilt and alignment differences between subjects, but leaving scale differences intact. To do this, each image volume was re-sliced into a standard orientation by a trained operator (A.L.) who "tagged" 20 standardized anatomical landmarks in each subject's image data set that corresponded to the same 20 anatomical landmarks defined on the ICBM-53 average brain (Mazziotta et al., 2001). Next, brain image volumes were more carefully spatially registered to *each other* by defining 144 standardized, manually defined anatomical landmarks (72 in each hemisphere, the first and last points on each of 36 sulcal lines drawn in each hemisphere described below) in every individual (Sowell et al., 2003; Thompson et al., 2005a,b). A least-squares, rigid-body transformation spatially matched each individual to the average of all the healthy controls. In this way, every individual's brain was matched in space, but global differences in brain size and shape remained intact. Landmarking was performed using MNI-Display software (Montreal Neurological Institute, Montreal, Canada) and was preferred relative to automated intensity-based registration, as cortical landmarks were available from a prior cortical thickness study (Thompson et al., 2005a,b).

Corpus callosum thickness maps

One rater (A.L.), blind to diagnosis, delineated the CC in the midsagittal section, as well as in 4 slices on either side of the midline (i.e., 9 slices total). This produced a 3D corpus callosum volume that extended 4 mm into each hemisphere. Structures were traced in serial sections using the software SEG (Laboratory of Neuro Imaging, University of California, Los Angeles), a segmentation editor that permits the delineation of regions of interest in images and stores them as ordered sets of boundary points. To assess inter-rater reliability, two independent investigators (A.L. and S.E.L.) contoured the CC from ten different randomly selected brains. The intraclass correlation coefficient obtained for total CC midsagittal area and volume were $r = 0.995$ and $r = 0.998$. Table 2 reports inter- and intrarater correlations for the volumes of structures traced in this study, as well as for volumes of the structure components.

To localize callosal thinning in AIDS, midsagittal callosal outlines were split, at the lowest points of the genu and splenium, into top and bottom segments as illustrated in Fig. 1. The digitized boundary points were then re-digitized to render them spatially uniform (Thompson et al., 1996a,b; Luders et al., in press; Vidal et al., submitted for publication). A medial curve threading down the CC was calculated by averaging spatially homologous boundary points on the top and bottom traces. At each of 100 equidistant points on the upper and lower traces, the distance to the medial line was computed and plotted on the upper and lower trace (Fig. 1).

Corpus callosum statistical maps

Thickness maps were averaged within each group (across corresponding points defined by the uniform parametric mesh), and group differences were assessed at each surface location by t tests. Mean group differences were plotted as a percentage reduction in local thickness. Regions with significant thickness differences (with $P < 0.05$) were coded in color (Fig. 4(c)). Within the AIDS group, local CC thickness was assessed for correlations with abnormal cognitive performance (as measured by the neurobehavioral exam), viral load, and CD4+ T cell counts. To do this, at each surface point, a multiple regression

Table 2
Intra-class correlations, from structures traced by two different image analysts, show high reliability within and between raters for area and volume measures

Structure	Inter-rater	Intra-rater
Corpus callosum area	0.995	0.995
Corpus callosum volume	0.998	0.998
Frontal horn volume	0.999	1.000
Occipital horn volume	0.996	0.997
Temporal horn volume	0.999	1.000

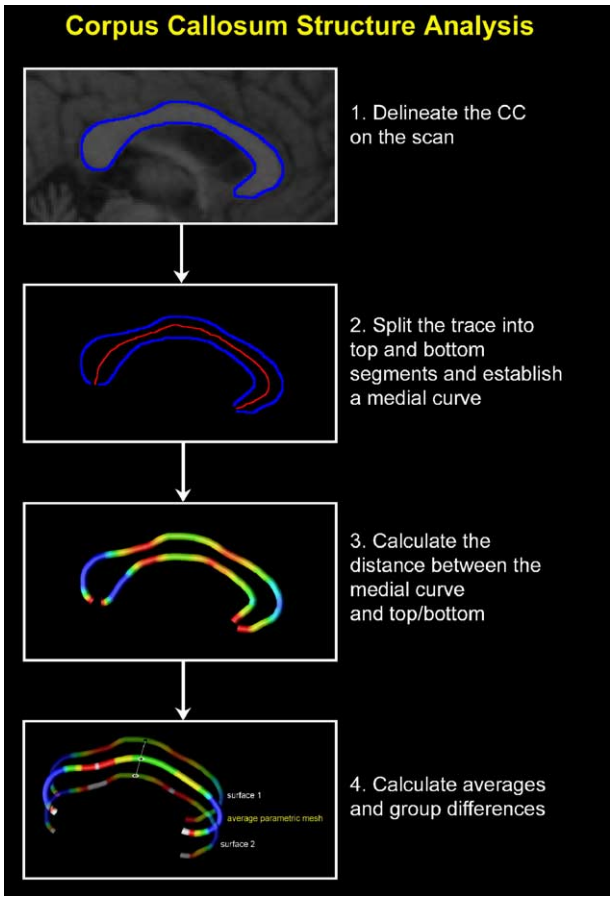

Fig. 1. Corpus callosum thickness maps. A flow chart shows how corpus callosum thickness is measured and averaged across a group of subjects. The corpus callosum is traced on a midsagittal section of each subject's MRI scan (1) and a medial curve is established that lies equidistant between the top and bottom traces [*red curve*; (2)]. The thickness of the CC is plotted as the distance of each boundary point from the medial curve ((3); other definitions are possible). Both the CC shape, and the thickness values, can be averaged across corresponding locations on the callosal boundary. Correspondence is defined here by using uniformly parameterized 2D curves and associating points at corresponding parameter locations (Thompson et al., 1998).

was run to assess whether the difference from the mean thickness at that point depended on the covariate of interest (e.g., group). The *P* value describing the significance of this linkage was plotted at each point on the CC using a color code to produce a statistical map. These maps reveal where the variable of interest is linked with structure. Overall *P* values were assigned to the maps using permutation testing (as in Thompson et al., 2004a,b). This avoids making assumptions about the spatial covariance of the residuals (Nichols and Holmes, 2002) and avoids complex parametric random field corrections (Thompson et al., 2004a,b). Although we did trace the CC in 3D, this did not provide better detection power than simply modeling it in 2D as a single midsagittal trace (Fig. 3). For simplicity, the corpus callosum thickness maps were therefore generated from the 2D traces in the midsagittal plane only. All color-coded maps in this study were created using the IBM Data Explorer visualization software, a general-purpose software package for data visualization and analysis (IBM T.J. Watson Research Center, New York; Abram and Treinish, 1995).

Ventricular shape and radial thickness mapping

To analyze ventricular shape, similar modeling steps were applied to the frontal, occipital and temporal horns of the lateral ventricles (delineation criteria are presented in Narr et al., 2001; see Fig. 2). Ventricles were manually traced bilaterally, converted into uniformly parameterized 3D surface meshes (Thompson et al., 2000), and 3D central curves were derived threading down the center of each of the three ventricular horns (illustrated in Fig. 2; Thompson et al., 2004a,b). Distance maps were computed indexing local expansion of the ventricular boundary from the medial curves in each subject. These surface-to-core radial distance fields were then averaged at corresponding surface locations across subjects and compared statistically between groups, at equivalent ventricular surface points in 3D space.

Ventricular statistical maps

Statistical maps were generated indicating local group differences in radial ventricular expansion and correlations with global cognitive impairment, T cell counts, and viral load. As for the CC, a multiple regression was run to assess whether the ventricular expansion at each surface point depended on the covariate of interest (e.g., T cell counts). The *P* value describing the significance of this linkage was plotted onto the surface at each point producing a color-coded statistical map (see Results for examples of these maps). These maps reveal where cognitive or immune system deficits link with expanding structure. Overall *P* values were assigned to the maps by permutation testing.

Brain size correction

No significant differences were found in total cerebral volume between patients and controls. Even so, we mapped AIDS-related differences in the corpus callosum and ventricles both *with and without* adjusting for effects of individual differences in brain size. Scaled maps and descaled maps were almost identical, and none of the significant results differed, so maps shown here were computed at their original scale in the brain (i.e., without scaling).

Results

Corpus callosum thickness maps

Fig. 3 shows the pattern of corpus callosum differences between AIDS patients and controls, using conventional morphometric measures, and Fig. 4 presents thickness differences identified using the mapping methods. As noted in Fig. 3(a), in this sample, total cerebral white matter was not significantly reduced overall, or in any lobe. CC volumes showed a trend for being lower in AIDS than in controls (by 10.7%; $P < 0.07$; Fig. 3(b)), and total midsagittal areas were significantly lower (by 11.5%; $P = 0.04$). To identify where thinning was greatest, we split the CC into five sectors along its anterior–posterior length, with the Witelson partitioning technique (Witelson, 1989; see Fig. 3(e) for how sectors are defined). Significant CC thinning was found in the anterior three sectors, where mean reductions ranged from 12.3 to 18.5%. Fig. 4 shows

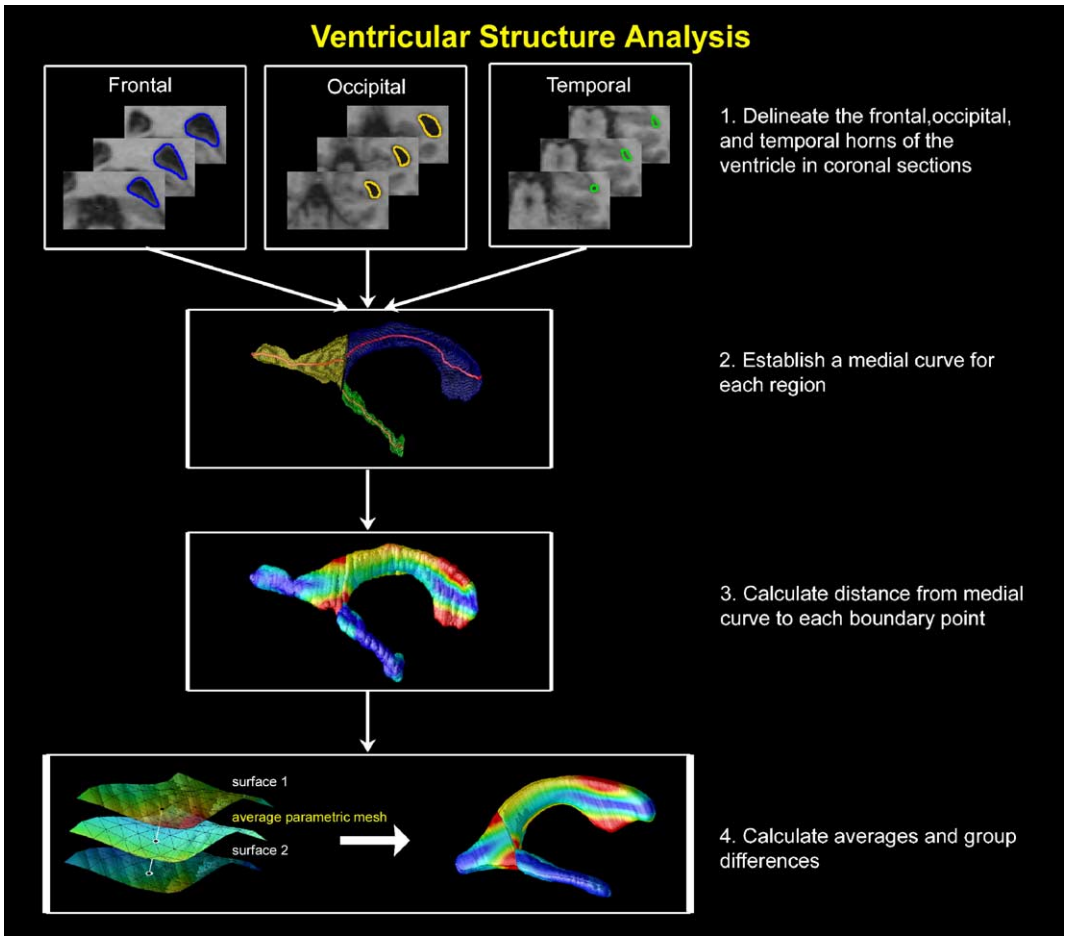

Fig. 2. Surface-based maps of lateral ventricle expansion. A flow chart shows how distance maps are used to measure ventricular expansion. The three horns (frontal, occipital, and temporal) of the lateral ventricles are traced manually in consecutive coronal sections, in images oriented into the ICBM standard space (1). Distance maps are computed (3) that specify the 3D distance of each ventricular surface point to a medial reference curve [*red curve*; (2)], that threads down the center of each component (Thompson et al., 2004). Red colors denote wider parts of the ventricles, blue colors denote thinner parts. A mesh averaging technique then averages surface models from different subjects. An average mesh can be created for a group of subjects, and the average distance from the centerline – for that group – is plotted at each surface point (4).

average maps of CC thickness in AIDS and in controls. The maps also reveal that frontal three sectors have the greatest thinning. In AIDS, the CC was up to 25% thinner ($P < 0.02$, *permutation test*), with greatest effect size in the anterior midbody and rostrum. In patients, the extent of CC thinning was also significantly linked with immune system decline measured by CD4+ T cell counts (Fig. 4(d); $P < 0.02$, *permutation test*). Those with greatest thinning in the CC midbody had greatest immunosuppression. Further supporting this association, T cell counts were significantly linked with CC areas in all the Witelson fifths ($P = 0.04$ for the posterior two sectors, $P < 0.009$ for the anterior three sectors), and they were also associated with the total midsagittal area of the CC, and with CC volume ($P < 0.008$; see Table 3 for details of the correlations with T cell counts). So, both maps and traditional measures suggested that CC thinning is associated with immune deterioration, especially in frontal sectors, even when no global white matter changes were detectable.

Ventricular volumes

Fig. 5 compares ventricular volumes in AIDS patients and controls. Total ventricular volumes were, on average, 2.18 times larger in AIDS than in controls ($P < 0.003$). Each hemisphere showed similar ventricular expansions (*left ventricle*: 2.19 times larger, $P < 0.002$; *right ventricle*: 2.16 times larger, $P < 0.004$). This expansion was not uniform, however. As shown in Fig. 5(b), the occipital horns were expanded by 171% (left) and 166% (right), while the temporal horns were only expanded by 66% and 73%, on the left and right (all $P < 0.05$). The frontal horns had an intermediate level of expansion (left: 111%, right: 107%; $P < 0.003$), but they had the greatest effect sizes, i.e., the mean differences were greatest as a proportion of their normal volumetric variance. In other words, the AIDS effect was easiest to detect in the frontal horns, even though the occipital horn expansion was proportionally greater.

3D ventricular maps

Fig. 6 shows the average ventricular shapes for the AIDS patients and healthy controls. In Fig. 6(b), the radial expansion of the ventricles in AIDS is expressed as a percentage relative to the expected values in controls. Red colors show that the greatest expansions (of 60%) are located on the caudate surfaces of the frontal horns and throughout the occipital horns. These expansions are highly significant (*frontal horn*: L, $P < 0.0002$, R, $P < 0.0003$;

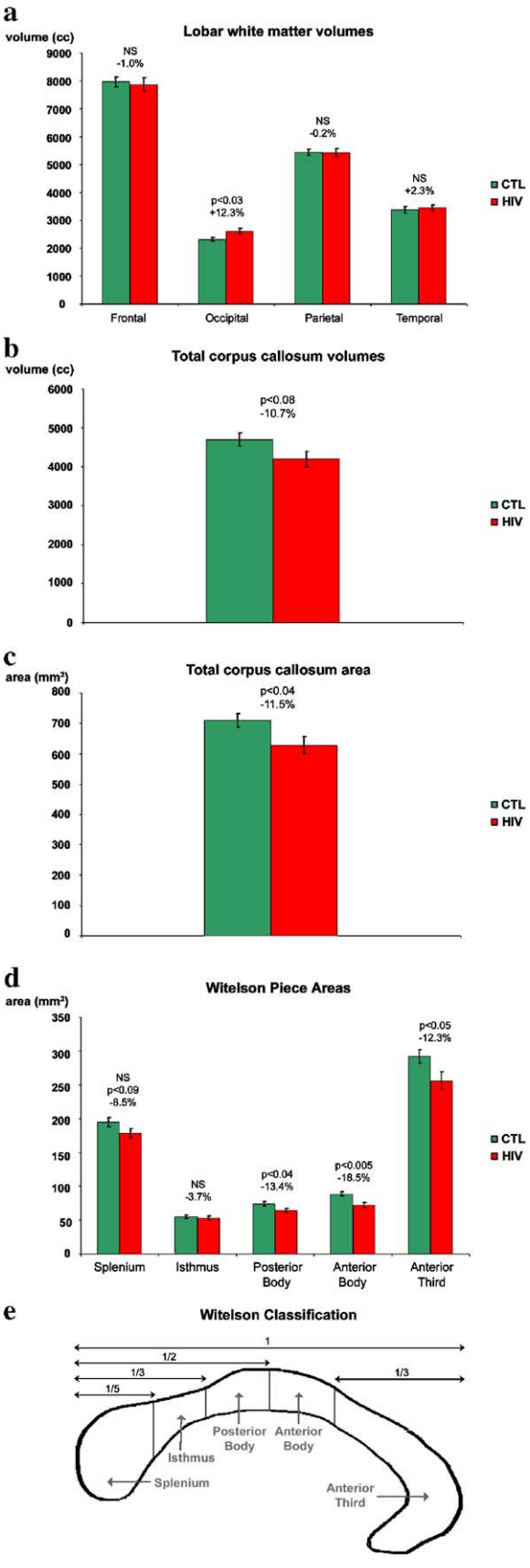

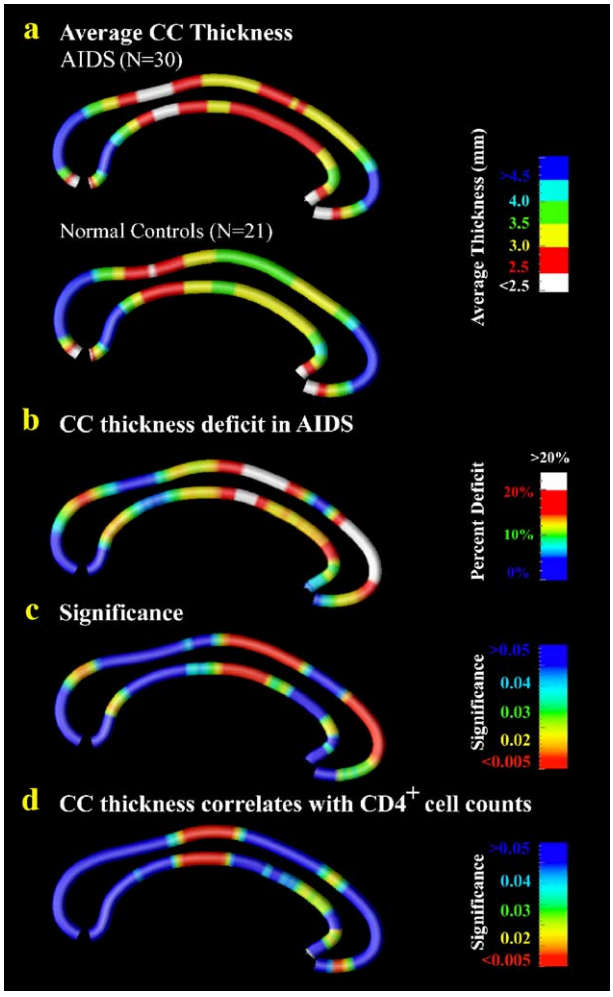

Fig. 4. Statistical maps of corpus callosum thickness. The average thickness of the CC is plotted in color on average CC shapes from HIV patients and controls (a). The average percent deficit in AIDS is shown plotted on a point-by-point basis. Reductions reach 25% in the frontal regions, agreeing with the more traditional Witelson measures (Fig. 3). These deficits are significant (c) and correlate with declining T cell counts (d), a measure of immune system integrity.

occipital horn: L, $P < 0.0002$, R, $P < 0.0009$). Based on visual inspection of the significance maps (Fig. 6(c)), the temporal horns appeared to offer the least power for detecting group differences, but expansions there were still significant on permutation testing (*temporal horn*: L, $P < 0.003$, R, $P < 0.008$).

Correlations with cognitive impairment and immune system deterioration

The level of ventricular expansion was correlated with global cognitive impairment, with greater expansion in impaired subjects

Fig. 3. Corpus callosum and related white matter measures in AIDS. Mean values for lobar white matter volumes (a), corpus callosum volumes (b), and corpus callosum cross-sectional areas are shown for healthy controls and AIDS patients. Error bars denote standard errors. When the CC is split into five sectors (d, e) using the partitioning technique defined by Witelson, greatest atrophy is found in the frontal three sectors. This is remarkable as no global or lobar white matter atrophy is detected (a) [diagram in panel e is adapted from Witelson, 1989].

Table 3
Corpus callosum areas and volume measures correlate with CD4+ T cell counts in the AIDS group

Measure	*P* value
Total CC area	0.005
Area: splenium	0.043
Area: isthmus	0.042
Area: posterior body	0.001
Area: anterior body	0.009
Area: anterior third	0.005
Total CC volume	0.008

This table shows the significance (*P* value) of correlations between various CC measures and CD4+ T cell counts, a measure of immune system integrity.

(Fig. 7). Effect sizes were greatest in the occipital horns (L, $P < 0.009$, R, $P < 0.009$). The degree of ventricular expansion was also significantly correlated with immune system decline measured by CD4+ T cell counts, with significance in the frontal and temporal horns (*frontal horn*: L, $P < 0.05$, R, $P < 0.04$; temporal horn: L: $P < 0.02$, R: $P < 0.02$) but only trend-level significance for the occipital horns (*occipital horn*: L, $P = 0.05$, R, $P = 0.07$). Interestingly, these associations with T cell counts were only found at trend-level if traditional volume measures rather than maps were used (*P* values between 0.05 and 0.1). Fig. 7(b) shows the diffuse anatomic profile of correlations between CD4+ T cell counts and ventricular expansion; as expected, worse immune function is linked with larger ventricles.

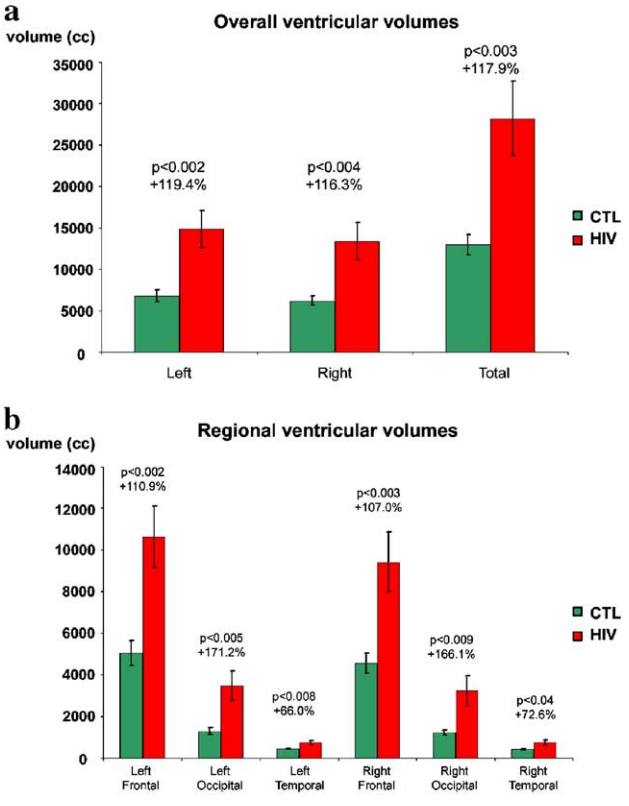

Fig. 5. Volume measures for lateral ventricle components. The volume of the lateral ventricles in AIDS is about 2.2 times its normal value, in both brain hemispheres (a). After splitting the ventricles into their three main components (frontal, occipital, and temporal), greatest expansion is found in the occipital horns, perhaps expanding in response to atrophy in the overlying parietal cortex.

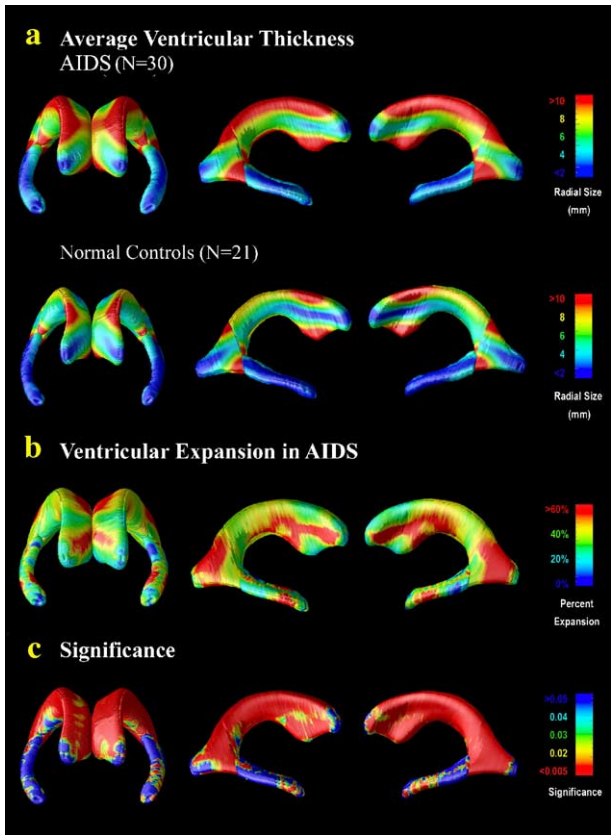

Fig. 6. Maps of ventricular expansion. The radial distance of each ventricular boundary point to a medial curve can be interpreted as "thickness" measure, as for the CC. Here, this measure is averaged across AIDS patients and, separately, across controls, and plotted on group average ventricular shapes. Red colors in the HIV group (a) indicate frontal horn expansions, relative to healthy controls. Panel b plots the ratio of the mean radial size in HIV versus controls, revealing regions with 60% expansion radially (*red colors*). Panel c shows the significance of these changes at each surface point. Changes in all three components are highly significant, even when corrected for multiple comparisons.

Discussion

This paper has two main findings. First, a pattern of thinning was detected throughout the CC in AIDS. In the frontal three-fifths of the CC, the deficit was as high as 25%. This thinning linked strongly with CD4+ T cell counts, a measure of immune system decline, and this association was found consistently with either mapping or traditional volumetry. CC white matter reductions do not simply reflect overall white matter atrophy, as cerebral white matter volumes were not reduced overall, in either hemisphere or in any lobe. White matter atrophy may therefore predominantly affect the CC, with frontal sectors affected the most. This pattern is somewhat opposite to the degenerative pattern seen at the CC in Alzheimer's disease, in which the isthmus is thinned most prominently (up to 25% in mild AD), presumably secondary to neurodegeneration in temporal and parietal cortices (Thompson et al., 1998, 2003). Because our AIDS cohort had no significant white matter

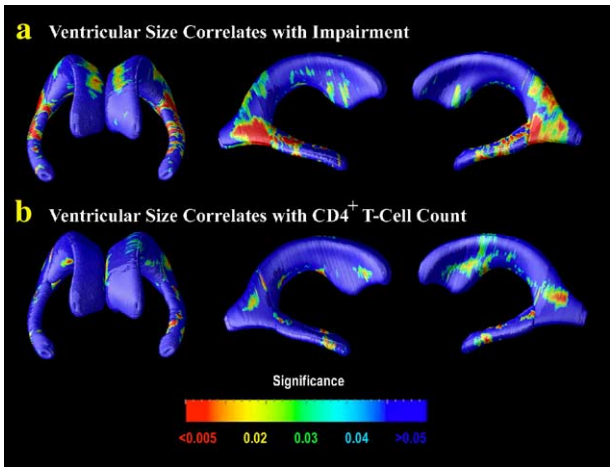

Fig. 7. Maps correlating ventricular expansion, cognition, and immunity. The maps show, in red, points where radial ventricular expansion links with cognitive impairment (a), and immune system integrity as measured by CD4+ T cell counts. Links appear weak but are significant after multiple comparisons correction. Only trend-level associations were found with traditional volume measures of the ventricles and their subcomponents.

reductions, white matter deficits may be easier to detect at midline than globally in AIDS. Jernigan et al. (2005) found that white matter volume was decreased in symptomatic HIV+ subjects, relative to comparison groups of asymptomatic HIV+ subjects, high-risk controls, and low-risk controls. However, this white matter atrophy may occur later in the disease than gray matter loss, or it may be more subtle, as suggested by other studies detecting gray but not white matter loss in AIDS (Di Sclafani et al., 1997). Measures of areas, volumes, and maps all detected a CC white matter deficit in AIDS, and all these measures were positively correlated with T lymphocyte counts, suggesting that they do track biological measures of disease burden. This supports the use of CC thickness as an MRI-based marker of white matter integrity in AIDS.

In a recent DTI study of 10 HIV patients (Filippi et al., 2001), the fractional anisotropy of water diffusion in the splenium was half its normal value and that in the genu was 25% decreased, with greatest decreases in advanced AIDS. In that study, the total diffusion constant in the frontal white matter was elevated (by 11%), perhaps reflecting a lack of myelin-based restriction of water diffusion, myelin damage, or astrogliosis. Ragin et al. (2004) also found that the whole brain fractional anisotropy was reduced and was associated with dementia severity, in 6 HIV patients, perhaps indicating worsening microscopic damage to white matter fiber tracts.

The mechanism of CC thinning in AIDS is of interest. In a recent study of cortical gray matter thickness in a subset of this cohort (Thompson et al., 2005a,b), the cortical regions with significant gray matter atrophy were anatomically restricted. Regions with 10–15% cortical atrophy extended from the sensorimotor and premotor cortex into the frontal eye fields in both brain hemispheres and posteriorly into parietal association cortices. The anterior CC primarily innervates frontal regions, and its midbody fibers project to sensorimotor regions, so selective CC atrophy may result from HIV-induced neuronal loss in these cortical regions. Pathological data suggest that there can be overt neuronal loss in AIDS, but it may be selective. Oster et al. (1995) and Fischer et al. (1999) detected an overall neuronal loss of 27% and 25% respectively (roughly 6×10^9 neurons) in the neocortex of AIDS patients. Larger neurons were most vulnerable, but neurodegeneration occurred in all lobes. Autopsy studies of AIDS patients with minor cognitive motor disorder (MCMD) reveal widespread loss of synapses (Wiley et al., 1991) and reduced dendritic complexity without overt neuronal loss. Other studies of MCMD reveal some cell loss in selected neuronal subpopulations, specifically in MAP-2 immunoreactive and calbindin pyramidal cells (Everall et al., 1993). It is perhaps surprising that we found such severe, CC deficits (25% thinning regionally) in this sample, as neuronal loss is thought to occur only in patients with more severe cognitive decline (e.g., in HIV-associated dementia) or who have CNS opportunistic infections, and these latter subjects were excluded from our study. McArthur et al. (1990) found that atrophy and leukoencephalopathy were common in AIDS, but in asymptomatic seropositive subjects, white matter changes were seen at only the same rate as in seronegative controls. Harrison et al. (1998) observed that white matter changes detected visually or by relaxometry were correlated with neuropsychological test scores in AIDS, independent of the presence of atrophy. Those with white matter changes performed more poorly on the Trail making test B, symbol digit tests, and non-verbal memory tests. In the Harrison et al. (1998) study, white matter T2 values were abnormally elevated in symptomatic relative to asymptomatic HIV+ subjects, but only frontal and parietal T2 increases were significant, consistent with the profile of cortical atrophy (Thompson et al., 2005a,b) and the predominantly anterior CC thinning seen here (see also Sardar et al., 1999, who studied altered frontal glutamate receptors in AIDS). In autopsy material from AIDS patients, leukoencephalopathy is often present, along with myelin pallor and astrocytosis. In principle, myelopathy may impair axonal conduction velocity and lead to psychomotor slowing, without necessarily implying extensive loss of cortical neurons. Even so, the profiles of cortical atrophy and CC thinning are likely to be causally linked.

Ventricular expansion is known to occur in AIDS, but here, we established its 3D pattern for the first time. The expansion was proportionally greatest in the occipital horns (2.7 times larger in AIDS). Frontal horn maps best distinguished patients from controls. These ventricular surfaces lie next to the caudate regions with greatest viral burden and were 2.1 times larger in AIDS than in controls. The temporal horns, which are only around 1.7 times larger in AIDS, provided poorest discrimination. Expansion in all these regions, assessed either with maps or volumetry, was significantly correlated with immune system integrity (measured by CD4+ T cell counts; $P < 0.04$) and with cognitive impairment ($P < 0.02$). This is consistent with older studies using 2D MRI measures, such as bicaudate/brain ratio (BCR) and bifrontal/brain ratio. Using those simpler measures, Hall et al. (1996) showed a correlation between increase in BCR and worsening neuropsychological performance over a 30-month time interval. In their study, the correlation held for both asymptomatic and symptomatic groups, with more pronounced changes in the symptomatic group.

Interestingly, our volumetric measures of ventricular regions detected only trend-level associations with CD4+ counts and impairment, suggesting that statistical maps may offer better detection sensitivity than volumes. As such, ventricular maps may be a useful biomarker of disease burden in AIDS, as they may mirror immunological measures of systemic decline. Ventricular expansion is usually a sign of diffuse atrophy in the brain, so these maps do not localize pathology in the conventional sense,

as might maps of gray matter structures such as the caudate, hippocampus, and cortex. The ventricles are relatively easy to measure though, so they are an attractive target for automated segmentation and labeling approaches (Carmichael et al., submitted for publication). Volumes and maps from well-validated, automated segmentations would be feasible to apply as an outcome measure of HAART efficacy in large-scale clinical trials. Although there is no doubt that 3D mapping will become an important tool for longitudinal trials, we should emphasize that, at this point, its future role in monitoring therapeutic effects is still speculative. In particular, the number of patients in this study is quite small, and the methods need to be validated in a large sample to better establish the practicality and power of the approach.

Our CC and ventricular maps linked well with T cell counts, and the ventricular measures reflected cognitive impairment, but none of our measures linked with viral load. There may be insufficient statistical power to detect a subtle association, but they may not correlate because viral load waxes and wanes in AIDS patients undergoing treatment. Only half of the patients in this study had detectable virus in plasma. Alternatively, atrophy and viral load may be associated, but only with a cerebral virus. The caudate nucleus, for example, exhibits significant atrophy in HIV and has the highest viral load (Stout et al., 1998). MRI-based measures of cortical gray matter also linked well with CD4+ counts but poorly with viral load (Thompson et al., 2005a,b). CC thinning and ventricular expansion, like T cell depletion, typically advance inexorably with longer duration of illness. They may progress over roughly the same stages of the illness, but longitudinal brain mapping studies are required to establish any dynamic relationship among them.

The surface-based modeling approach employed here extends our earlier research (Thompson et al., 1996a,b, 2004a,b) and is related to other ongoing work using medial representations (*M-reps*; Styner et al., 2004, 2005), spherical harmonics (Thompson and Toga, 1996; Gerig et al., 2001), or high-dimensional deformation mapping of anatomical surfaces (Joshi et al., 1997; Csernansky et al., 2004, 2005). Shape and computational mapping approaches have been most commonly applied to the hippocampus, revealing the anatomical changes in normal brain development (Gogtay et al., 2005), schizophrenia (Narr et al., 2001), Alzheimer's disease and other dementias (Thompson et al., 2004a,b; Frisoni et al., submitted for publication), epilepsy (Lin et al., in press), autism (Nicolson et al., submitted for publication), and mild cognitive impairment (Becker et al., in press, submitted for publication).

In some studies, surface-based maps may offer greater statistical power than traditional volumetric measures. Here, both approaches detected essentially similar effects, but we found moderate evidence that maps were more powerful. The maps revealed a significant association of ventricular expansion with T cell counts and cognitive impairment, whereas volume measures in the same regions only found trend-level correlations (albeit in the same direction). In general, surface-based modeling may outperform traditional volumetry, especially when resolving shape alterations that do not affect a structure uniformly, or in detecting highly localized effects (see, for example, Thompson et al., 2005a,b).

As demonstrated here, brain mapping may help in understanding the 3D profile of anatomical deficits associated with HIV infection. Statistical anatomic maps are more complex than traditional volumetric measures, but they may help in monitoring treatment and offer possible end points in drug trials. In the past, clinical trials of anti-retroviral compounds – such as zidovudine and didanosine – have used brain measures as a surrogate marker of HIV disease progression (see Englund et al., 1997). Mapping techniques may also help, as they can localize where associations are strongest between structural brain changes and systemic measures, such as T cell counts and (in principle) viral load.

This study also has some limitations, which will be alleviated in future. Manual interaction with images is time consuming, and as such, this analysis technique is not yet automated enough to be used as a surrogate end-point for clinical studies of HIV cognitive dysfunction. We are currently validating deformable atlas algorithms to identify surfaces automatically using manual traces as a gold standard (Carmichael et al., submitted for publication), and these approaches offer greater automation and higher throughput of images. This study is also cross-sectional. Longitudinal studies mapping disease progression will better establish the trajectory of the changes observed here (cf. Thompson et al., 2004a,b; Leow et al., 2005, for related longitudinal brain maps in development and dementia). Masliah et al. (1992) hypothesized that HIV infection spreads in the brain by first entering the striatum via the ventricles and then spreading along white matter tracts into the cortex. It would be interesting to determine, using longitudinal MRI, whether the spatial trajectory of atrophy lends any support to this hypothesis.

Before claims of regionally specific atrophy can be made for the CC, it is important to assess whether there are spatial variations in factors that affect the detection power, such as the

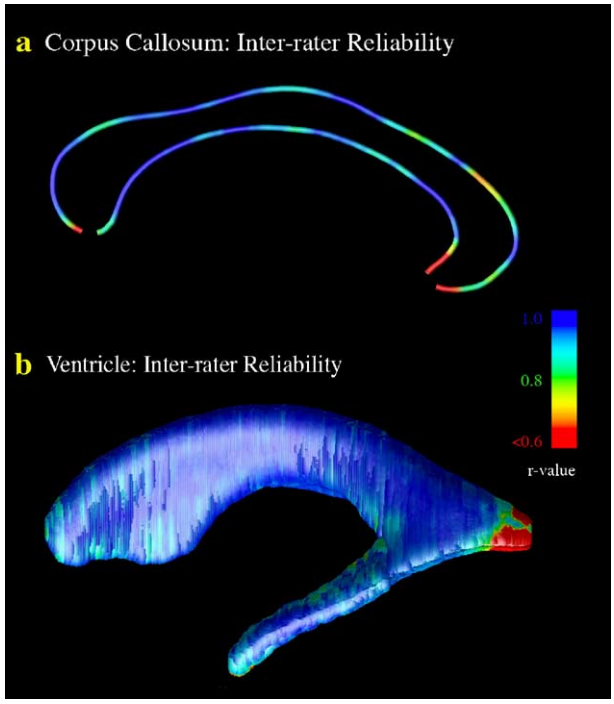

Fig. 8. Intraclass correlation maps show manual traces are reliable. The CC and ventricles were traced independently in 10 brains by two different raters following the same anatomical protocol. As in Thompson et al. (2004a,b), a way to reveal disagreement between tracers is to plot the intraclass correlation in the form of a map, by running a regression at each surface vertex for the surface parameters (CC thickness and ventricular expansion). Reliability is high except at the occipital horn tips, which are small and hard to distinguish on MRI (see also Table 2).

inter-rater reliability. Non-uniform spatial sensitivity is common in brain mapping studies, but the 3D profile of errors has rarely been mapped in morphometric studies. Fig. 8(a) shows the inter-rater correlation for thickness measures, based on two image analysts each tracing 10 CC outlines blindly and independently. When these correlations are presented in the form of a map, some regions with lowest reliability (ICC < 0.9; Fig. 8(a)) were among those where significant group differences were detected. This is rather paradoxical, as it would be more logical to expect reduced detection power in regions with poorer inter-rater reliability, as the error variance would increase. Comparing Fig. 4(c) with Fig. 8(a), reliability in identifying structures may have been slightly poorer in regions where greatest effect sizes were detected in this study (e.g., where the average thinning reaches 20%). Any non-uniform profile of inter-rater reliability could introduce a spatial bias (non-uniform sensitivity) in the results. The detected correlations between thinning and CD4+ T cell counts may also be compared to the ICC maps, although high CD4 correlations were found in regions with relatively good and relatively poorer reliability (reliability was worst in regions with very small thickness values, e.g., near the anterior commissure; Fig. 8(a)). Maps of segmentation errors such as these can be plotted for 3D surfaces as well as planar curves (Fig. 8(b)). If the errors are unbiased and truly random (as would be expected in a blinded study), it may improve statistical power to use rater averages.

With developments in image analysis, data such as these are soon likely to be processed more rapidly and on a larger scale. As well as revealing systems most prominently affected by HIV, neuroimaging biomarkers may soon be widely employed to measure therapeutic effects in clinical trials of neuroprotective compounds (such as memantine, deprenyl, etc.) (Nath et al., 2000), as well as for monitoring disease progression in individual patients.

Acknowledgments

This research was supported by the National Institute on Aging (AG021431 to JTB and AG016570 to PMT), the National Library of Medicine, the National Institute for Biomedical Imaging and Bioengineering, and the National Center for Research Resources (LM05639, EB01651, RR019771 to PMT). JTB was the recipient of a Research Scientist Development Award–Level II (MH01077).

References

Abram, G., Treinish, L., 1995. An extended data-flow architecture for data analysis and visualization. Proceedings of the IEEE Visualization 1995 Conference, October 1995, pp. 263–270.

Archibald, S.L., Masliah, E., Fennema-Notestine, C., Marcotte, T.D., Ellis, R.J., McCutchan, J.A., Heaton, R.K., Grant, I., Mallory, M., Miller, A., Jernigan, T.L., 2004. Correlation of in vivo neuroimaging abnormalities with postmortem human immunodeficiency virus encephalitis and dendritic loss. Arch. Neurol. 61, 369–376.

Becker, J.T., Lopez, O.L., Dew, M.A., Aizenstein, H.J., 2004. Prevalence of cognitive disorders differs as a function of age in HIV virus infection. AIDS 18 (Suppl. 1), S11–S18.

Becker, J.T., Davis, S.W., Hayashi, K.M., Meltzer, C.C., Lopez, O.L., Toga, A.W., Thompson, P.M., in press. 3D patterns of hippocampal atrophy in mild cognitive impairment. Neurology (to appear Jan. 2006).

Becker, J.T., Hayashi, K.M., Seaman, J.L., Lopez, O.L., Aizenstein, H.J., Toga, A.W., Thompson, P.M., submitted for publication. Alteration in hippocampal and caudate nucleus structure in HIV/AIDS revealed by three dimensional mapping.

Carmichael, O.T., Thompson, P.M., Dutton, R.A., Lu, A., Lee, S.E., Lee, J.Y., Aizenstein, H.A., Meltzer, C.C., Liu, Y., Becker, J.T., submitted for publication. Fully-automated segmentation of HIV-dilated ventricles.

Center for Disease Control, 1992. 1993 Revised classification system for HIV infection and expanded case definition for AIDS among adolescents and adults. Morb. Mort. Wkly. Rep. 41 (RR-17), 1–19.

Chang, L., Lee, P.L., Yiannoutsos, C.T., Ernst, T., Marra, C.M., Richards, T., Kolson, D., Schifitto, G., Jarvik, J.G., Miller, E.N., Lenkinski, R., Gonzalez, G., Navia, B.A., HIV MRS Consortium, 2004. A multicenter in vivo proton-MRS study of HIV-associated dementia and its relationship to age. NeuroImage 23 (4), 1336–1347 (Dec.).

Csernansky, J.G., Wang, L., Joshi, S.C., Ratnanather, J.T., Miller, M.I., 2004. Computational anatomy and neuropsychiatric disease: probabilistic assessment of variation and statistical inference of group difference, hemispheric asymmetry, and time-dependent change. NeuroImage 23 (Suppl. 1), S56–S68 (Review).

Csernansky, J.G., Wang, L., Swank, J., Miller, J.P., Gado, M., McKeel, D., Miller, M.I., Morris, J.C., 2005. Preclinical detection of Alzheimer's disease: hippocampal shape and volume predict dementia onset in the elderly. NeuroImage 25 (3), 783–792 (Apr. 15).

Cummings, J.L., Mega, M., Gray, K., 1994. The Neuropsychiatric Inventory: comprehensive assessment of psychopathology in dementia. Neurology 44, 2308–2314.

Cysique, L.A., Maruff, P., Brew, B.J., 2004. Antiretroviral therapy in HIV infection: are neurologically active drugs important? Arch. Neurol. 61, 1699–1704.

Derogatis, L., 1992. The Brief Symptom Inventory (BSI): Administration, Scoring and Procedures Manual (Clinical Psychometric Research, Baltimore Research).

Di Sclafani, V., Mackay, R.D., Meyerhoff, D.J., Norman, D., Weiner, M.W., Fein, G., 1997. Brain atrophy in HIV infection is more strongly associated with CDC clinical stage than with cognitive impairment. J. Int. Neuropsychol. Soc. 3, 276–287 (May).

Englund, J.A., Baker, C.J., Raskino, C., McKinney, R.E., Petrie, B., Fowler, M.G., Pearson, D., Gershon, A., McSherry, G.D., Abrams, E.J., Schliozberg, J., Sullivan, J.L., 1997. Zidovudine, didanosine, or both as the initial treatment for symptomatic HIV-infected children. AIDS Clinical Trials Group (ACTG) Study 152 Team. N. Engl. J. Med. 336 (24), 1704–1712 (Jun. 12).

Ernst, T., Chang, L., 2004. Effect of aging on brain metabolism in antiretroviral-naive HIV patients. AIDS 18 (Suppl. 1), S61–S67 (Jan. 1).

Everall, I., Luthert, P., Lantos, P., 1993. A review of neuronal damage in human immunodeficiency virus infection: its assessment, possible mechanism and relationship to dementia. J. Neuropathol. Exp. Neurol. 52, 561–566.

Fahn, S., Elton, R.L., 1987. Unified Parkinson's disease rating scale. In: Fahn, S., Marsden, C.D., Goldstein, M., et al., (Eds.), Recent Developments in Parkinson's Disease. Macmillan, Florham Park.

Filippi, C.G., Ulug, A.M., Ryan, E., Ferrando, S.J., van Gorp, W., 2001. Diffusion tensor imaging of patients with HIV and normal-appearing white matter on MR images of the brain. Am. J. Neuroradiol. 22 (2), 277–283 (Feb.).

Fischer, C.P., Jorgen, G., Gundersen, H., Pakkenberg, B., 1999. Preferential loss of large neocortical neurons during HIV infection: a study of the size distribution of neocortical neurons in the human brain. Brain Res. 15, 119–126.

Frisoni, G., Sabattoli, F., Lee, A.D., Dutton, R.A., Toga, A.W., Thompson, P.M., submitted for publication. In vivo neuropathology of the hippocampal formation in the degenerative dementias: a radial mapping study.

Gerig, G., Styner, M., Shenton, M.E., Lieberman, J., 2001. Shape versus size: Improved understanding of the morphometry of brain structures. MICCAI 2001: Fourth International Conference on Medical Image

Computing and Computer-Assisted Intervention, Utrecht, The Netherlands, Springer LNCS 2208, pp. 24–32 (October 14–17).

Gogtay, N., Nugent, T.F., Herman, D.H., Ordonez, A., Greenstein, D., Hayashi, K.M., Clasen, L., Toga, A.W., Giedd, J.N., Rapoport, J.L., Thompson, P.M., 2005. Dynamic Mapping of Normal Human Hippocampal Development. (revised for Cereb. Cortex).

Hall, M., Whaley, R., Robertson, K., Hamby, S., Wilkins, J., Hall, C., 1996. The correlation between neuropsychological and neuroanatomic changes over time in asymptomatic and symptomatic HIV-1-infected individuals. Neurology 46 (6), 1697–1702 (Jun.).

Harrison, M.J., Newman, S.P., Hall-Craggs, M.A., Fowler, C.J., Miller, R., Kendall, B.E., Paley, M., Wilkinson, I., Sweeney, B., Lunn, S., Carter, S., Williams, I., 1998. Evidence of CNS impairment in HIV infection: clinical, neuropsychological, EEG, and MRI/MRS study. J. Neurol., Neurosurg. Psychiatry 65 (3), 301–307 (Sep.).

Heaton, R.K., 1981. Wisconsin Card Sorting Manual. Psychological Assessment Resources, Odessa.

Hestad, K., McArthur, J.H., Dal Pan, G.J., Selnes, O.A., Nance-Sproson, T.E., Aylward, E., Mathews, V.P., McArthur, J.C., 1993. Regional brain atrophy in HIV-1 infection: association with specific neuropsychological test performance. Acta Neurol. Scand. 88 (2), 112–118 (Aug.).

Heyes, M.P., Ellis, R.J., Ryan, L., Childers, M.E., Grant, I., Wolfson, T., Archibald, S., Jernigan, T.L., 2001. Elevated cerebrospinal fluid quinolinic acid levels are associated with region-specific cerebral volume loss in HIV infection. Brain 124 (Pt. 5), 1033–1042 (May).

Jernigan, T.L., Gamst, A.C., Archibald, S.L., Fennema-Notestine, C., Mindt, M.R., Marcotte, T.D., Heaton, R.K., Ellis, R.J., Grant, I., 2005 (Aug.). Effects of methamphetamine dependence and HIV infection on cerebral morphology. Am. J. Psychiatry 162 (8), 1461–1472.

Joshi, S.C., Miller, M.I., Grenander, U., 1997. On the geometry and shape of brain submanifolds. Intl. J. of Pattern Recognition and Artificial Intelligence 11, 1317–1343.

Kieburtz, K., Ketonen, L., Cox, C., Grossman, H., Holloway, R., Booth, H., Hickey, C., Feigin, A., Caine, E.D., 1996. Cognitive performance and regional brain volume in human immunodeficiency virus type 1 infection. Arch. Neurol. 53 (2), 155–158 (Feb.).

Langford, T.D., Letendre, S.L., Larrea, G.J., Masliah, E., 2003. Changing patterns in the neuropathogenesis of HIV during the HAART era. Brain Pathol. 13 (2), 195–210.

Lawton, M.P., Brody, E.M., 1969. Assessment of older people: self-maintaining and instrumental activities of daily living. Gerontologist 9, 179–186.

Leow, A.D., Huang, S.C., Geng, A., Becker, J.T., Davis, S.W., Toga, A.W., Thompson, P.M., 2005. Inverse Consistent Mapping in 3D Deformable Image Registration: Its Construction and Statistical Properties, Information Processing in Medical Imaging (IPMI) 2005, Glenwood Springs, Colorado, July 11–15, 2005.

Levy, R.M., Bredesen, D.E., Rosenblum, M.L., 1986. Neurological manifestations of the acquired immunodeficiency syndrome (AIDS): experience at UCSF and review of the literature. J. Neurosurg. 62, 475–495.

Lin, J.J., Salamon, N., Lee, A.D., Dutton, R.A., Geaga, J.A., Hayashi, K.M., Toga, A.W., Engel, J., Thompson, P.M., in press. 3D preoperative maps of hippocampal atrophy maps predict surgical outcomes in temporal lobe epilepsy, Neurology.

Luders, E., Narr, K.L., Zaidel, E., Thompson, P.M., Jancke, L., Toga, A.W., in press. Parasagittal asymmetries of the corpus callosum Cereb. Cortex (electronic publication ahead of print).

Masliah, E., Ge, N., Achim, C.L., Hansen, L.A., Wiley, C.A., 1992. Selective neuronal vulnerability in HIV encephalitis. J. Neuropathol. Exp. Neurol. 51 (6), 585–593 (Nov.).

Mazziotta, J.C., Toga, A.W., Evans, A.C., Fox, P.T., Lancaster, J., Zilles, K., Woods, R.P., Paus, T., Simpson, G., Pike, B., Holmes, C.J., Collins, D.L., Thompson, P.M., MacDonald, D., Schormann, T., Amunts, K., Palomero-Gallagher, N., Parsons, L., Narr, K.L., Kabani, N., Le Goualher, G., Boomsma, D., Cannon, T., Kawashima, R., Mazoyer, B., 2001. A probabilistic atlas and reference system for the human brain (Invited Paper). J. R. Soc. 356 (1412), 1293–1322.

McArthur, J.C., Kumar, A.J., Johnson, D.W., et al., 1990. Incidental white matter hyperintensities on magnetic resonance imaging in HIV-1 infection. Multicentre AIDS cohort study. J. Acquired Immune Defic. Syndr. 3, 252–259.

Narr, K.L., Thompson, P.M., Sharma, T., Moussai, J., Blanton, R.E., Anvar, B., Edris, A., Krupp, R., Rayman, J., Khaledy, M., Toga, A.W., 2001. 3D shape characterization and mapping of temporo-limbic regions and the lateral ventricles in schizophrenia. Biol. Psychiatry 50 (2), 84–97 (July 15).

Narr, K.L., Thompson, P.M., Szeszko, P., Robinson, D., Jang, S., Woods, R.P., Kim, S., Hayashi, K.M., Asunction, D., Toga, A.W., Bilder, R.M., 2004. Regional specificity of hippocampal volume reductions in first episode schizophrenia. NeuroImage 21 (4), 1563–1575 (Apr.).

Nath, A., Haughey, N.J., Jones, M., Anderson, C., Bell, J.E., Geiger, J.D., 2000. Synergistic neurotoxicity by human immunodeficiency virus proteins Tat and gp120: protection by memantine. Ann. Neurol. 47, 186–194.

Navia, B.A., Gonzalez, R.G., 1997. Functional imaging of the AIDS dementia complex and the metabolic pathology of the HIV-1-infected brain Review. Neuroimaging Clin. N. Am. 7 (3), 431–445 (Aug.).

Neuenburg, J.K., Brodt, H.R., Herndier, B.G., Bickel, M., Bacchetti, P., Price, R.W., Grant, R.M., Schlote, W., 2002. HIV-related neuropathology, 1985 to 1999: rising prevalence of HIV encephalopathy in the era of highly active antiretroviral therapy. J. Acquired Immune Defic. Syndr. 31, 171–177.

Nichols, T.E., Holmes, A.P., 2002. Nonparametric permutation tests for functional neuroimaging: a primer with examples. Hum. Brain Mapp. 15 (1), 1–25 (Jan.).

Nicolson, R., DeVito, T., Vidal, C.N., Sui, Y., Hayashi, K.M., Drost, D.J., Williamson, P.C., Rajakumar, N., Toga, A.W., Thompson, P.M., submitted for publication. Detection and Mapping of Hippocampal Abnormalities in Autism.

Oster, S., Christoffersen, P., Gundersen, H.J., Nielsen, J.O., Pedersen, C., Pakkenberg, B., 1995. Six billion neurons lost in AIDS. A stereological study of the neocortex. APMIS 103, 525–529.

Patel, S.H., Kolson, D.L., Glosser, G., et al., 2002. Correlation between percentage of brain parenchymal volume and neurocognitive performance in HIV-infected patients. Am. J. Neuroradiol. 23, 543–549.

Pomara, N., Crandall, D.T., Choi, S.J., Johnson, G., Lim, K.O., 2001. White matter abnormalities in HIV-1 infection: a diffusion tensor imaging study. Psychiatry Res. 106, 15–24.

Ragin, A.B., Storey, P., Cohen, B.A., Epstein, L.G., Edelman, R.R., 2004. Whole brain diffusion tensor imaging in HIV-associated cognitive impairment. Am. J. Neuroradiol. 25 (2), 195–200 (Feb.).

Rottenberg, D.A., Sidtis, J.J., Strother, S.C., Schaper, K.A., Anderson, J.R., Nelson, M.J., Price, R.W., 1996. Abnormal cerebral glucose metabolism in HIV-1 seropositive subjects with and without dementia. J. Nucl. Med. 37 (7), 1133–1141 (Jul.).

Sacktor, N., Van Heertum, R.L., Dooneief, G., Gorman, J., Khandji, A., Marder, K., Nour, R., Todak, G., Stern, Y., Mayeux, R., 1995. A comparison of cerebral SPECT abnormalities in HIV-positive homosexual men with and without cognitive impairment. Arch. Neurol. 52 (12), 1170–1173 (Dec.).

Sacktor, N., McDermott, M.P., Marder, K., Schifitto, G., Selnes, O.A., McArthur, J.C., Stern, Y., Albert, S., Palumbo, D., Kieburtz, K., De Marcaida, J.A., Cohen, B., Epstein, L., 2002. HIV-associated cognitive impairment before and after the advent of combination therapy. J. NeuroVirol. 8 (2), 136–142 (Apr.).

Sardar, A.M., Hutson, P.H., Reynolds, G.P., 1999. Deficits of NMDA receptors and glutamate uptake sites in the frontal cortex in AIDS. NeuroReport 10, 3513–3515.

Sowell, E.R., Peterson, B.S., Thompson, P.M., Welcome, S.E., Henkenius, A.L., Toga, A.W., 2003. Mapping cortical change across the human life span. Nat. Neurosci. 6 (3), 309–315.

Spitzer, R.L., Williams, J.B., Gibbon, M., et al., 1989. Instruction manual for the Structured Clinical Interview for DSM-III-R (Biometrics Research, New York State Psychiatric Institute, New York).

Stout, J.C., Archibald, S.L., Jernigan, T.L., et al., 1998. HIV Neurobehavioral Research Center Group. Progressive cerebral volume loss in human immunodeficiency virus infection: a longitudinal volumetric magnetic resonance imaging study. Arch. Neurol. 55, 161–168.

Styner, M., Lieberman, J.A., Pantazis, D., Gerig, G., 2004. Boundary and medial shape analysis of the hippocampus in schizophrenia. Med. Image Anal. 8 (3), 197–203 (Sep.).

Styner, M., Lieberman, J.A., McClure, R.K., Weinberger, D.R., Jones, D.W., Gerig, G., 2005. Morphometric analysis of lateral ventricles in schizophrenia and healthy controls regarding genetic and disease-specific factors. Proc. Natl. Acad. Sci. U. S. A. 102 (13), 4872–4877 (Mar. 29).

Thompson, P.M., Toga, A.W., 1996. A surface-based technique for warping 3-dimensional images of the brain. IEEE Trans. Med. Imaging 15 (4), 1–16 (August).

Thompson, P.M., Schwartz, C., Lin, R.T., Khan, A.A., Toga, A.W., 1996a. 3D statistical analysis of sulcal variability in the human brain. J. Neurosci. 16 (13), 4261–4274.

Thompson, P.M., Schwartz, C., Toga, A.W., 1996b. High-resolution random mesh algorithms for creating a probabilistic 3D surface atlas of the human brain. NeuroImage 3 (1), 19–34 (March).

Thompson, P.M., Moussai, J., Khan, A.A., Zohoori, S., Goldkorn, A., Mega, M.S., Small, G.W., Cummings, J.L., Toga, A.W., 1998. Cortical variability and asymmetry in normal aging and Alzheimer's disease. Cereb. Cortex 8 (6), 492–509 (Sept.).

Thompson, P.M., Mega, M.S., Narr, K.L., Sowell, E.R., Blanton, R.E., Toga, A.W., 2000. Brain image analysis and atlas construction, invited chapter. In: Fitzpatrick, M., Sonka, M. (Eds.), SPIE Handbook on Medical Image AnalysisSociety of Photo-Optical Instrumentation Engineers (SPIE) Press, pp. 1063–1131.

Thompson, P.M., Hayashi, K.M., de Zubicaray, G., Janke, A.L., Rose, S.E., Semple, J., Herman, D., Hong, M.S., Dittmer, S., Doddrell, D.M., Toga, A.W., 2003. Dynamics of gray matter loss in Alzheimer's disease. J. Neurosci. 23 (3), 994–1005.

Thompson, P.M., Hayashi, K.M., de Zubicaray, G., Janke, A.L., Rose, S.E., Semple, J., Hong, M.S., Herman, D., Gravano, D., Doddrell, D.M., Toga, A.W., 2004. Mapping hippocampal and ventricular change in Alzheimer's disease. NeuroImage 22 (4), 1754–1766 (Aug. 2004; published online, June 1, 2004).

Thompson, P.M., Hayashi, K.M., Simon, S., Geaga, J., Hong, M.S., Sui, Y., Lee, J.Y., Toga, A.W., Ling, W.L., London, E.D., 2004b. Structural abnormalities in the brains of human subjects who use methamphetamine. J. Neurosci. 24 (26), 6028–6036 (June 30).

Thompson, P.M., Hayashi, K.M., Sowell, E.R., et al., 2004c. Mapping cortical change in Alzheimer's disease, brain development, and schizophrenia. NeuroImage 23 (Suppl. 1), S2–S18.

Thompson, P.M., Dutton, R.A., Hayashi, K.M., Toga, A.W., Lopez, O.L., Aizenstein, H.J., Becker, J.T., 2005a. Thinning of the cerebral cortex visualized in HIV/AIDS reflects CD4+ T-lymphocyte decline, 102 (43) 15647–15652 (October 25, 2005 published online, Oct. 10, 2005).

Thompson, P.M., Lee, A.D., Dutton, R.A., Geaga, J.A., Hayashi, K.M., Eckert, M.A., Bellugi, U., Galaburda, A.M., Korenberg, J.R., Mills, D.L., Toga, A.W., Reiss, A.L., 2005b. Abnormal cortical complexity and thickness profiles mapped in Williams syndrome. J. Neurosci. 25 (16), 4146–4158 (Apr. 20).

Thurnher, M.M., Schindler, E.G., Thurnher, S.A., Pernerstorfer-Schon, H., Kleibl-Popov, C., Rieger, A., 2000. Highly active antiretroviral therapy for patients with AIDS dementia complex: effect on MR imaging findings and clinical course. Am. J. Neuroradiol. 21 (4), 670–678 (Apr.).

UNAIDS, 2004. AIDS Epidemic Update: December 2004. http://www.unaids.org/wad2004/report_pdf.html.

Vidal, C.N., DeVito, T.J., Nicolson, R., Hayashi, K.M., Geaga, J.A., Drost, D.J., Williamson, P.C., Rajakumar, N., Sui, Y., Dutton, R.A., Toga, A.W., Thompson, P.M., submitted for publication. Mapping Corpus Callosum Deficits in Autistic Disorder.

Wang, L., Swank, J.S., Glick, I.E., Gado, M.H., Miller, M.I., Morris, J.C., Csernansky, J.G., 2003. Changes in hippocampal volume and shape across time distinguish dementia of the Alzheimer type from healthy aging. NeuroImage 20 (2), 667–682 (Oct.).

Wiley, C.A., Masliah, E., Morey, M., et al., 1991. Neocortical damage during HIV infection. Ann. Neurol. 29, 651–657.

Witelson, S.F., 1989. Hand and sex differences in the isthmus and genu of the human corpus callosum. Brain 112, 799–835.